

Complementary inchworm[®] actuator for high-force high-precision applications

David F. Waechter^{*a}, Shaun Salisbury^b, Ridha Ben Mrad^b
S. Eswar Prasad^a, Richard G. Blacow^a, and Bin Yan^a

^aSensor Technology Limited, PO Box 97, Collingwood, ON Canada L9Y 3Z4

^bDepartment of Mechanical and Industrial Engineering, University of Toronto, 5 King's College Rd
Toronto, Canada M5S 3G8

ABSTRACT

An inchworm actuator is described which uses complementary configurations for the two clamping sections. In one configuration clamping and release are achieved using high and low voltage respectively while for the other clamping and release are achieved using low and high voltage respectively. The resulting inchworm actuator can be driven by a two-channel controller with the two clamps sharing the first channel and the extender piezoelectric actuator using the second channel. In the coarse positioning mode the direction of motion is determined by whether the extender voltage pulse overlaps the leading or trailing edge of the common clamp pulse. A fine positioning mode can be realized with the common clamp voltage set to 0V and continuous feedback control applied to the extender actuator. The paper also describes a diode-shunted delay circuit that causes unclamping to occur more slowly than clamping. It is shown that by using the delay circuit in series with each clamp, the overall force drive capability of the actuator is increased. The paper presents simulated and experimental results of clamp surface displacement and force vs. time during the switching transient.

Keywords: complementary, inchworm, actuator, piezoelectric

1. INTRODUCTION

Inchworm actuators are devices that achieve long range motion by rapidly repeating a clamp-extend-clamp cycle¹. They typically use two piezoelectric actuators for two clamp sections and a third for the extender section². Magnetostrictive³, electrostrictive⁴ or electrostatic⁵ actuation have also been proposed for the clamp or extender sections. In the coarse positioning mode the clamp and extender sections are activated in the required sequence by a 3-channel controller. A fine positioning mode can also be realized by activating the extender section under continuous feedback control while one clamp is on and the other is released.

While hybrid inchworm actuators have been proposed in which the clamp and extender sections use different actuation technologies³, it is most often the case that the two clamp sections use the same actuation technology in an identical configuration. In this work we propose the use of complementary clamps in which one clamp grips with low voltage and releases with high voltage while the other is released with low voltage and grips with high voltage. These will be referred to as normally clamped (NC) and normally unclamped (NU) respectively. It will be shown that by using complementary clamps it is possible to drive the inchworm actuator with a 2-channel controller with the two clamps sharing a common channel. It is also possible to enter the fine positioning mode with both clamps unpowered. The paper also describes a diode-shunted RLC circuit, which when placed in series with each clamp, slows the rate of unclamping relative to clamping. It will be shown that the circuit increases the holding force of the two clamps during the switching transient, thereby increasing the overall force drive capability of the actuator.

®Inchworm is a registered trademark of Burleigh Instruments Inc.

*dwaechter@sensortech.ca; phone 1 705 444-1440 ext. 29; fax 1 705 444-6787; www.sensortech.ca

The complementary clamps in the new inchworm actuator are analogous to complementary transistors in CMOS (complementary metal-oxide-semiconductor) circuits. CMOS n and p-channel transistors share a common gate and turn on with positive and negative gate voltage respectively⁶. These circuits dissipate significant power only during the switching transient and this is also true of the complementary clamps with associated RLC circuit. While ion implantation may be used to adjust the threshold voltage of CMOS transistors, it will be shown that simple mechanical adjustment provides similar control of the clamping threshold voltage of the complementary clamps described here.

Section 2 describes the general concept of complementary inchworm actuation and introduces some clamp designs with adjustable clamping thresholds. Section 3 describes the delay circuit and explains its operation. Section 4 then presents the dynamic model used in simulations and Section 5 presents both simulated and experimental results. In Section 6, an analysis of the results and an assessment of the force drive capability of the inchworm actuator are presented. Conclusions are summarized in Section 7.

2. ACTUATOR CONCEPT

Two general configurations of linear complementary inchworm actuators are shown in Fig. 1. We refer to that of Fig 1a) as the NU actuator and that of Fig. 1b) as the NC actuator. These designations can be thought of as referring to the clamp type that is able to move relative to the actuator frame. However when applied to the overall inchworm actuator it is more appropriate to interpret NC and NU as meaning normally controlled and normally uncontrolled respectively. In the NU actuator with unpowered clamps ($V=0$), the moving member is rigidly clamped with respect to the actuator frame and activation of the extender section has no effect on the position of the member. In the NC actuator with unpowered clamps, the position of the moving member can be finely controlled by extender activation. The NU actuator can also enter a fine positioning mode but requires high DC voltage on the clamps to do so. The panels on the right side of Fig. 1 show the common clamp and extender signals that advance the moving member in the direction indicated in the coarse positioning mode. The direction of motion is determined by whether the extender signal overlaps the leading or trailing edge of the common clamp signal.

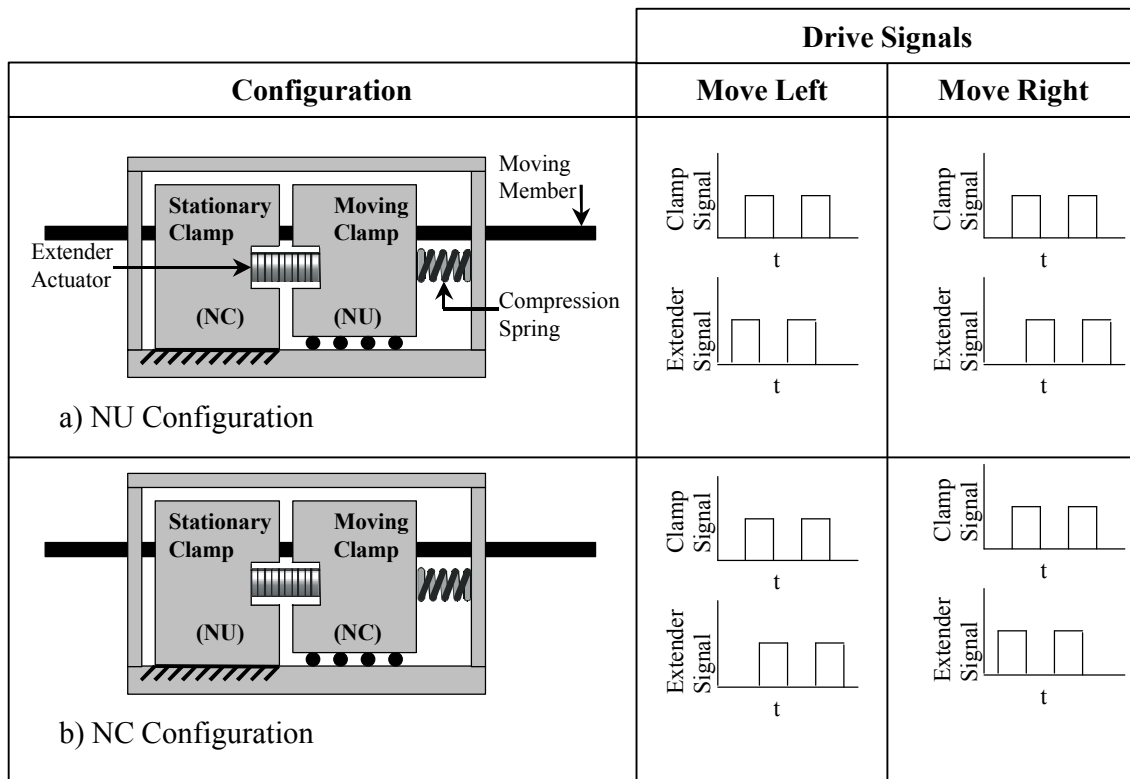


Figure 1. Complementary inchworm actuator configurations and their required drive signals.

Design configurations for the NU and NC clamps are illustrated in Fig. 2 along with the corresponding restraining force vs. applied voltage characteristics. For the NU clamp of Fig. 2a) a multilayer piezoelectric stack is supported in a flexure frame in order to maintain a moderate pre-stress and protect the stack from shear forces imparted by the moving member. An upper clamping surface is suspended above the moving member and held in place by front and back face-plates (not shown in the figure). The upper section of the clamp has a relatively stiff flexure and a less stiff internal spring that can be compressed by set-screw rotation. Because of the low stiffness ratio between the internal spring and upper flexure, the position of the unobstructed upper clamping surface can be adjusted with micron level control by set-screw rotation. The NU clamp is adjusted so that with zero voltage on the piezoelectric stack the gap between the two clamping surfaces slightly exceeds the moving member thickness, resulting in zero clamping force. The clamping threshold voltage V_{TNU} is the piezoelectric stack voltage at which the separation of the two clamping surfaces first equals the moving member thickness. It can be adjusted by set-screw rotation. Beyond V_{TNU} the restraining force on the moving member begins to rise. The subsequent slope of the restraining force vs. voltage characteristic depends on the properties of the piezoelectric stack, the stiffness of the upper clamping flexure and the coefficient of friction between the moving member and clamping surfaces. The force F_{maxNU} denotes the maximum restraining force, corresponding to the maximum permissible applied voltage for the stack actuator.

Fig. 2b) shows a possible configuration for the NC clamp. It is essentially the same as the NU clamp of Fig. 2a) except that the piezoelectric stack is oriented to use d_{31} contraction with applied positive voltage rather than d_{33} expansion. However because the magnitude of d_{31} is generally less than d_{33} for piezoelectric materials, a substantially taller stack would be needed to obtain comparable performance to the NU counterpart. Fig 2c) shows an alternative design that overcomes this difficulty. The form of the restraining force vs. applied voltage characteristic for both of these designs is shown in the right panel of Figs. 2b) and 2c). As with the NU counterpart the threshold voltage V_{TNC} can be adjusted by rotating the set-screw in the upper flexure.

Fig. 2d) shows a third NC design in which a piezoelectric stack is used to raise a horizontal bar that clamps on the top of the moving member. This design uses the same flexure frame to house the piezoelectric stack as in the lower portion Fig 2a), but the frame is now shown in side view. The clamping force F_{maxNC} at $V=0$ is established by using the adjustment bolt with compression spring while the central contact piece is in a raised position. The contact piece can then be locked into contact with the actuator frame with the stack voltage set equal to the value V_0 . The slope of the descending portion of the restraining force vs. applied voltage characteristic depends on the properties of the piezoelectric stack, the compliance of the horizontal bar and the relevant coefficient of friction.

3. DELAY CIRCUIT

When the two clamps in a complementary inchworm actuator are switching state there will be no point in time when both clamps exert zero restraining force on the moving member, provided the condition $V_{TNC} > V_{TNU}$ is satisfied. There will however be a time period when the total restraining force acting on the moving member (ie. $F_{NU} + F_{NC}$) is less than either F_{maxNU} or F_{maxNC} . In the special case when the switching time is very short this may have minimal impact on the actuator performance, since the moving member will not have sufficient time to slip. We note for example that if the moving member were able to move for 0.1 ms and started from rest while subject to the acceleration of gravity, it would move a distance of only 49 nm. This is small compared to the typical step size of an inchworm actuator (usually several microns or more). However for slower clamp switching speeds a complementary inchworm actuator using a single clamp channel would have a lower force drive capability than if the same actuator used two clamp channels to ensure that one clamp achieved maximum force before the other began to release. A complementary inchworm actuator with 2-channel control can nevertheless approach 3-channel performance by using a suitable delay circuit that causes the unclamping operation to occur more slowly than clamping. One such delay circuit is described qualitatively here and is analyzed quantitatively in subsequent sections.

Fig. 3 shows the delay circuit connected to each clamp with a common voltage supply. The circuit assumes subresonant operation where the piezoelectric stack actuators can be modeled as simple capacitors having values C_{NU} and C_{NC} . The

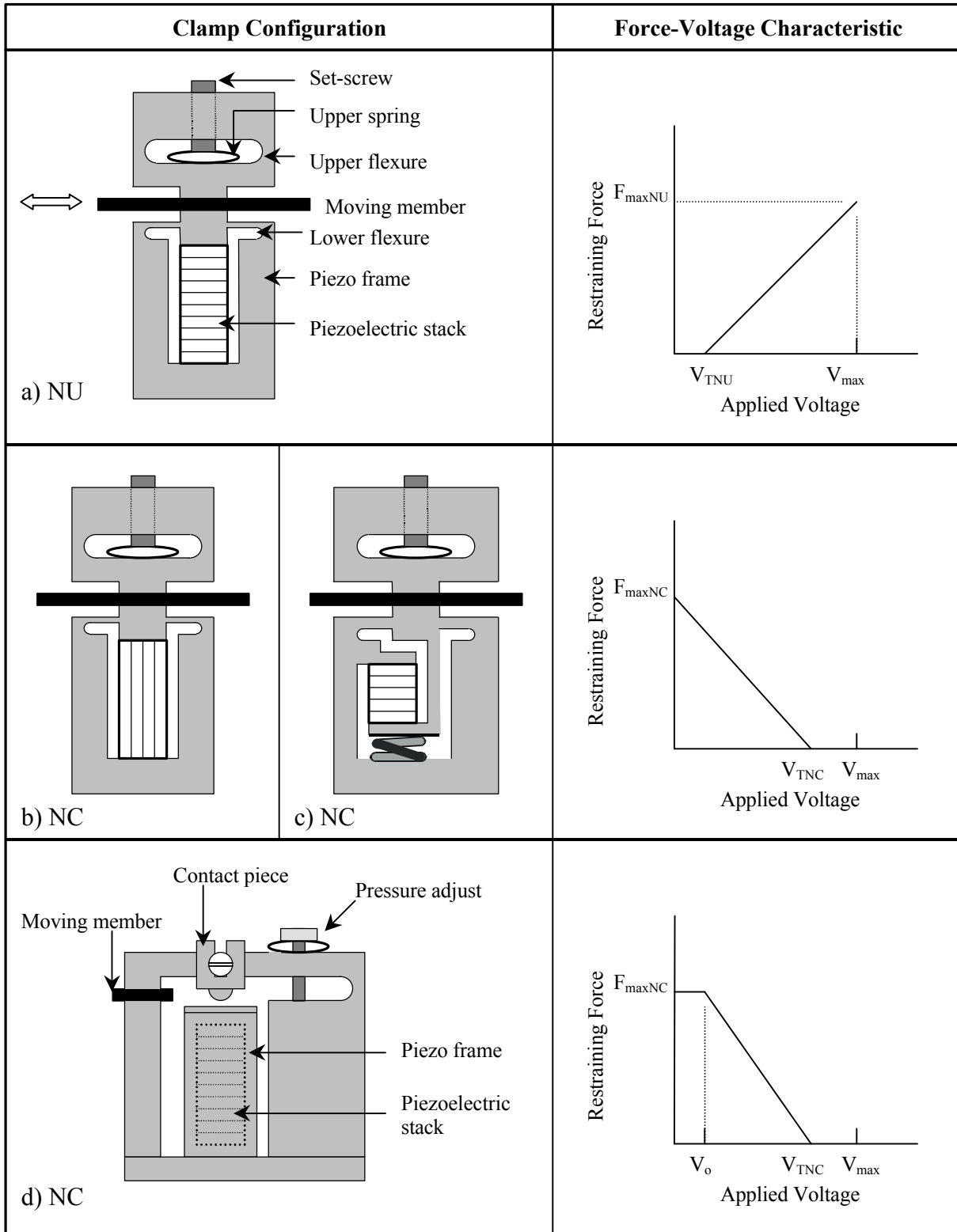


Figure 2. Complementary inchworm actuator clamp configurations and their corresponding force-voltage characteristics, a) NU configuration and b), c) & d) different NC configurations.

stack actuators considered in this work have area 5x5mm, height 11mm and a low frequency capacitance of approximately 400 nF. The displacement of the stacks at the rated maximum voltage (200V) is just over 12 μm . A diode-shunted RLC circuit is placed in series with each clamp. The diodes are pointed in different directions so that for each clamp type the RLC circuit is bypassed during the clamping operation. In this case the clamp voltage closely follows the input signal. However during unclamping the diode is reverse biased and behaves as an open circuit. The RLC circuit can now influence the output voltage and slows its average ramp rate relative to the input signal.

In the case where the RLC circuit is not bypassed, the delay circuit operation for one of the clamp branches can be explained as follows. In steady-state the RL branch discharges the capacitor C thereby ensuring that the actuator voltage $V_{\text{NC,NU}}$ equals the input voltage V_{in} . Also in steady-state, zero current will flow through the resistor R, so that there is no stand-by power dissipation in R. When the input voltage first begins to change from a constant value, current will flow exclusively through the capacitor C since the current through an inductor cannot change instantaneously. In this initial period the circuit of a single clamp branch will appear to the voltage source as two capacitors in series. The voltage will change less rapidly across the larger capacitor and, for this reason, we choose $C \ll C_{\text{NU,NC}}$. However once the inductor begins to pass significant current, it will tend to discharge C and bring the output voltage close to the input voltage. In order to prevent oscillation, the resistor R should be larger than the critical value $R=2[L/(C+C_{\text{NU,NC}})]^{1/2}$. The effect of various R values on the circuit performance is examined in Sections 5 and 6.

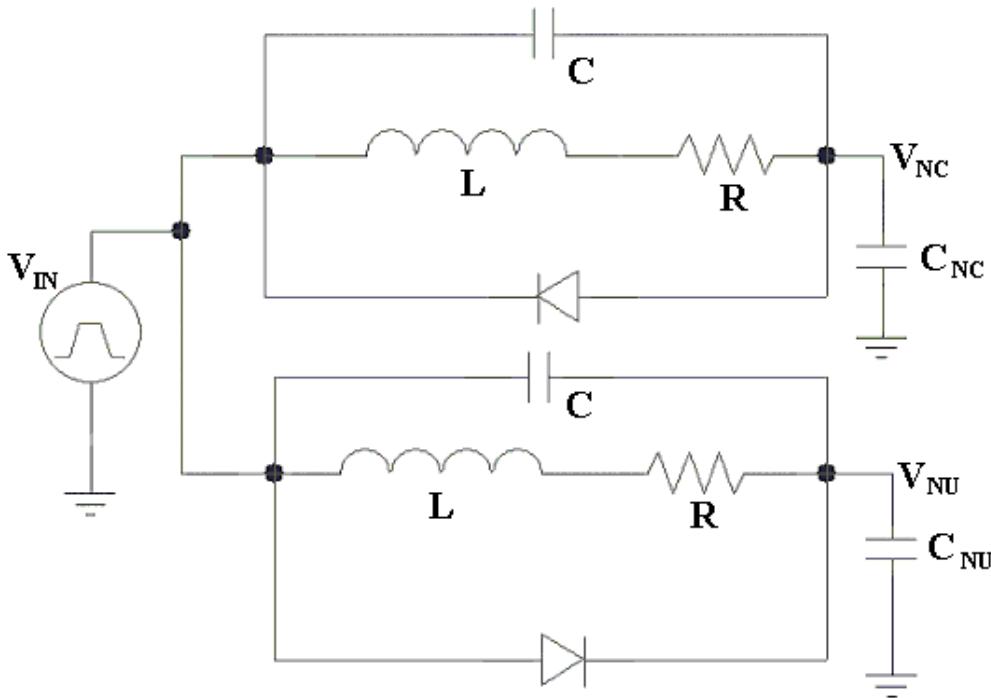


Figure 3. Circuit used to slow the rate of unclamping in NU and NC clamps of complementary inchworm actuator.

4. DYNAMIC MODEL

The dynamic model of the clamp is composed of coupled electrical and mechanical sub-models. The mechanical model for the NU clamp from Fig. 2a) is considered because it is the basis of the other clamp types. The clamp can be represented as shown in Fig. 4. The piezoelectric stack, upper spring, lower flexure and upper flexure have stiffnesses k_p , k_s , k_f and k_{fa} respectively. The lower flexure has a clearance, C_r , to the moving member at $V=0$. The clamping force, F_c , is the net result of the piezoelectric stack force, F_p , and the lower flexure force, F_f .

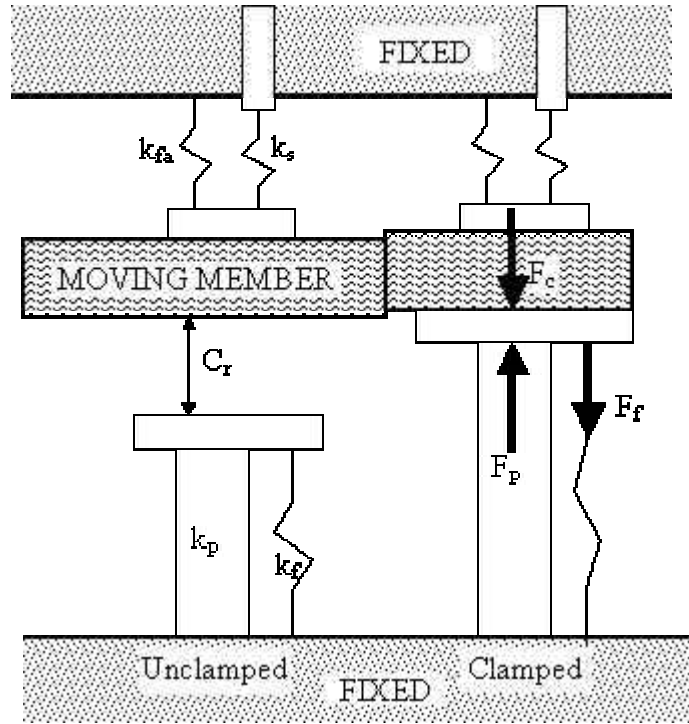


Figure 4. NU clamp representation in the unclamped ($V=0$) and clamped ($V>V_{TNU}$) states.

Using equations developed previously⁷, the clamping force can be calculated as a function of input voltage and initial clearance:

$$F_c = \begin{cases} \frac{k_s + k_{fa}}{k_p + k_f + k_s + k_{fa}} \left(k_p \frac{L_0}{V_0} V - (k_p + k_f) C_r \right) & \text{for } V > V_{TNU} \\ 0 & \text{for } V \leq V_{TNU} \end{cases} \quad (1)$$

The threshold voltage, V_{TNU} , is given by:

$$V_{TNU} = \frac{C_r (k_p + k_f)}{L_0 k_p} V_{\max} \quad (2)$$

L_0 is the free expansion of the piezoelectric stack at maximum voltage V_{\max} . These equations give the relationship of the Force-Voltage characteristic in Fig. 2a) where F_c and the restraining force F_{NU} are related by the coefficient of friction. Clamping force is easier to consistently measure than the restraining force which is why it is considered here. The maximum clamping force which can be realized is:

$$F_{c_{MAX}} = \frac{k_s + k_{fa}}{k_p + k_f + k_s + k_{fa}} (k_p L_0 - (k_p + k_f) C_r) \quad (3)$$

These equations are based on a static analysis and neglect hysteresis. The combination of the stiffnesses and masses involved in motion result in a very small mechanical time constant, and therefore the clamping force follows the clamp voltage profile without significant lag.

The clamp voltages are related to the input voltage by the following transfer function which depends on whether the diode or the RLC portion of the circuit is active:

$$V_{NU,NC} = \begin{cases} \frac{s^2 CL + sCR + 1}{s^2 L(C + C_{NU,NC}) + sR(C + C_{NU,NC}) + 1} V_{IN} & ; RLC \text{ circuit active} \\ V_{IN} & ; diode \text{ active} \end{cases} \quad (4)$$

PSPICE⁸ was used to simulate the voltage applied to the piezoelectric stacks using the model shown in Fig. 3. Given the values for C, L, R, C_{NC} and C_{NU}, the voltages across C_{NC} and C_{NU} were determined. These voltages were then used with equations (1) and (2) to determine the force output of the actuator.

5. RESULTS

Tests were conducted on a prototype clamp with diode-shunted delay circuit to assess the displacement and force behavior. The piezo frame with stack actuator (lower section of Fig. 2a) was mounted in a test fixture and the base secured. For the initial unrestrained tests, a capacitive position sensor was used to measure the displacement of the clamping surface as a function of time. We note that when used in the NU configuration of Fig. 2a, stack expansion causes an increase of restraining force, while when used in the NC configuration, such as Fig. 2d, stack expansion causes a decrease of restraining force. The voltage signal was generated by an arbitrary waveform generator. The signal passed through an amplifier and into the diode-shunted delay circuit which controlled the clamp. The voltage signal profile was a step with ramped edges at a frequency of 200 Hz. The input voltage and displacement were monitored in real time using a digital sampling oscilloscope.

Figures 5 and 6 show the input voltage signal and the measured displacement for two different diode orientations. The diode orientation for Fig. 5 is appropriate to the NC clamp while that of Fig. 6 is appropriate to the NU clamp. The delay circuit parameter values were L=1mH, C=100nF and R=750Ω. The figure shows how the displacement significantly lags the input voltage on one side of the voltage pulse, but follows more closely on the other.

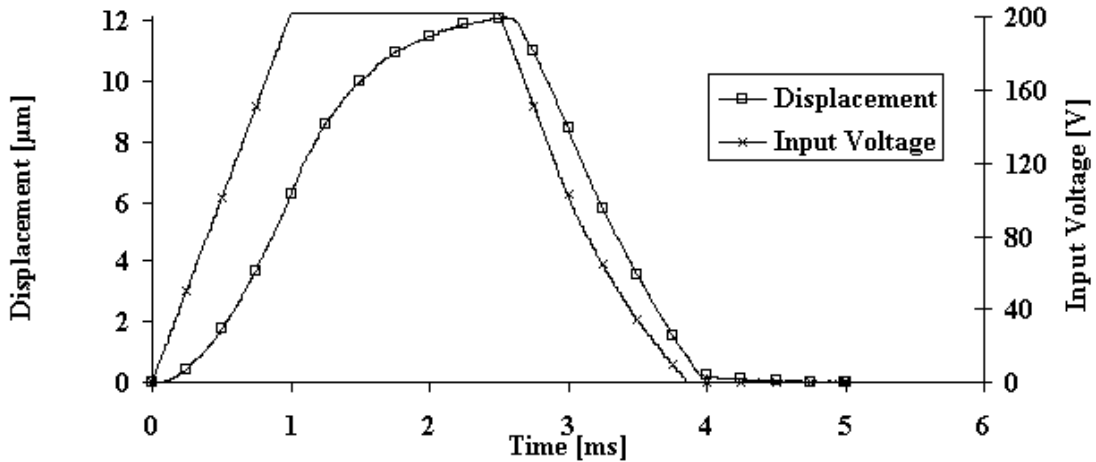


Figure 5. Input voltage and measured displacement vs. time with diode oriented to bypass delay circuit on the falling edge, as required for NC configuration clamp.

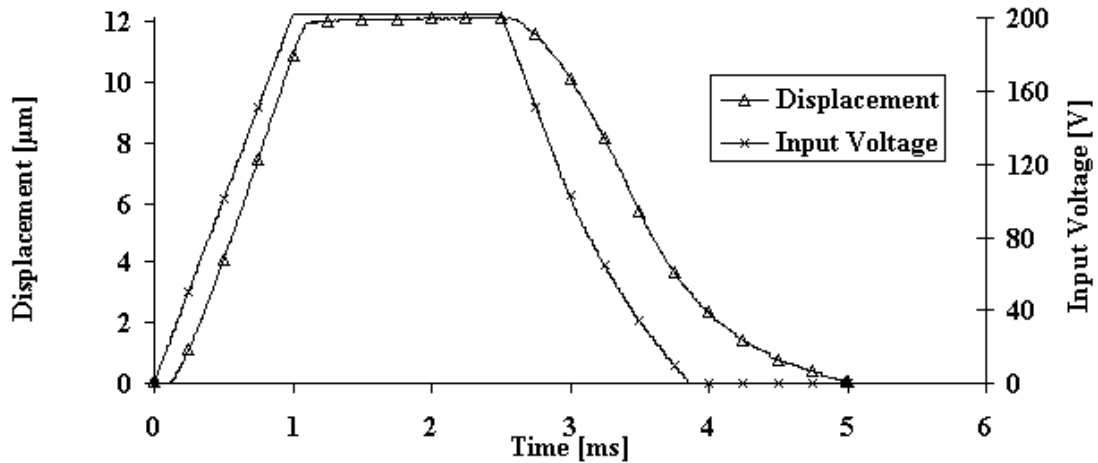


Figure 6. Input voltage and measured displacement vs. time with diode oriented to bypass delay circuit on the rising edge, as required for NU configuration clamp.

Blocked tests were also conducted on the lower portion of the NU clamp of Fig. 2a. A quartz load cell with a stiffness of $1000 \text{ N}/\mu\text{m}$ was placed on top of the clamp surface. A thick steel bar was slid into contact on the other side and tightened along its length to provide a rigid structure. This meant that the clearance C_r and the clamping threshold voltage V_{TNU} were set to zero for this particular measurement, even though a practical inchworm actuator would normally use small positive values for these quantities. The sum of k_s+k_{fa} was assumed infinite for computational purposes. The same voltage profile was input into the system and the clamp force instead of the displacement was measured. Figures 7 and 8 show simulated and experimental results of the NU clamping force for various RL branch resistances. Both figures show that the rate of force reduction is reduced by the delay circuit and that greater R reduces the rate of reduction by a larger amount. The model and the measurements are in good agreement.

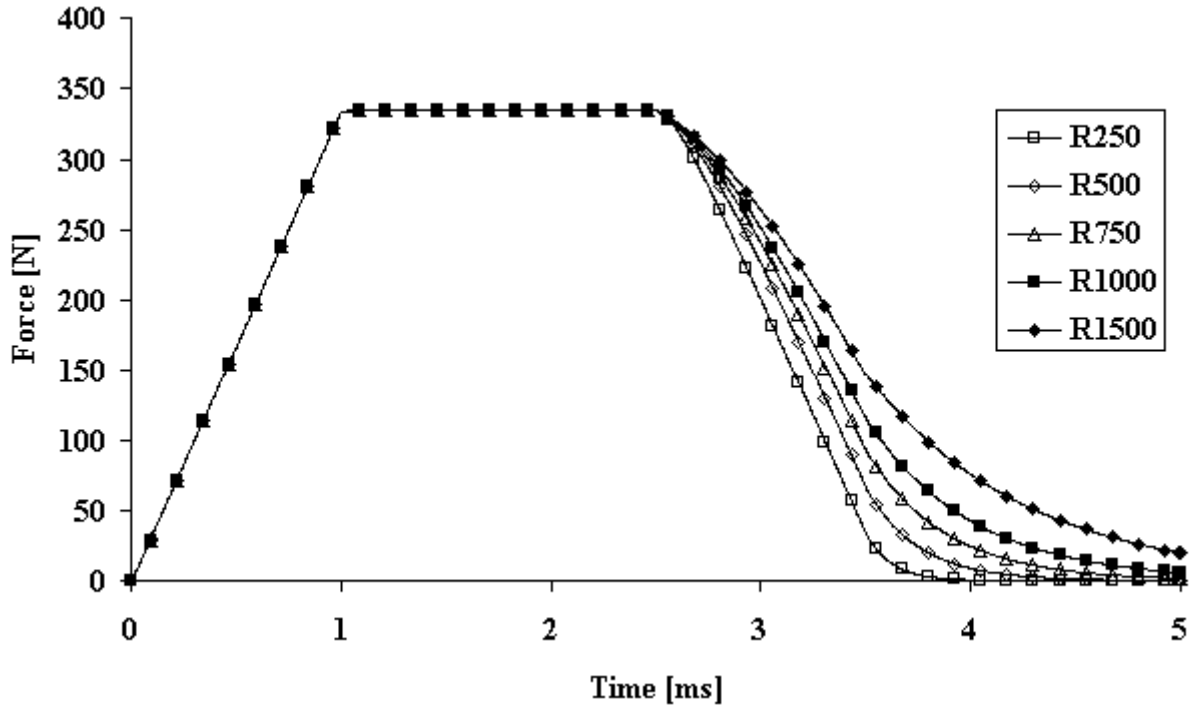


Figure 7. Simulation results showing clamping force vs. time for various resistances in the delay circuit acting on the falling edge of the voltage input.

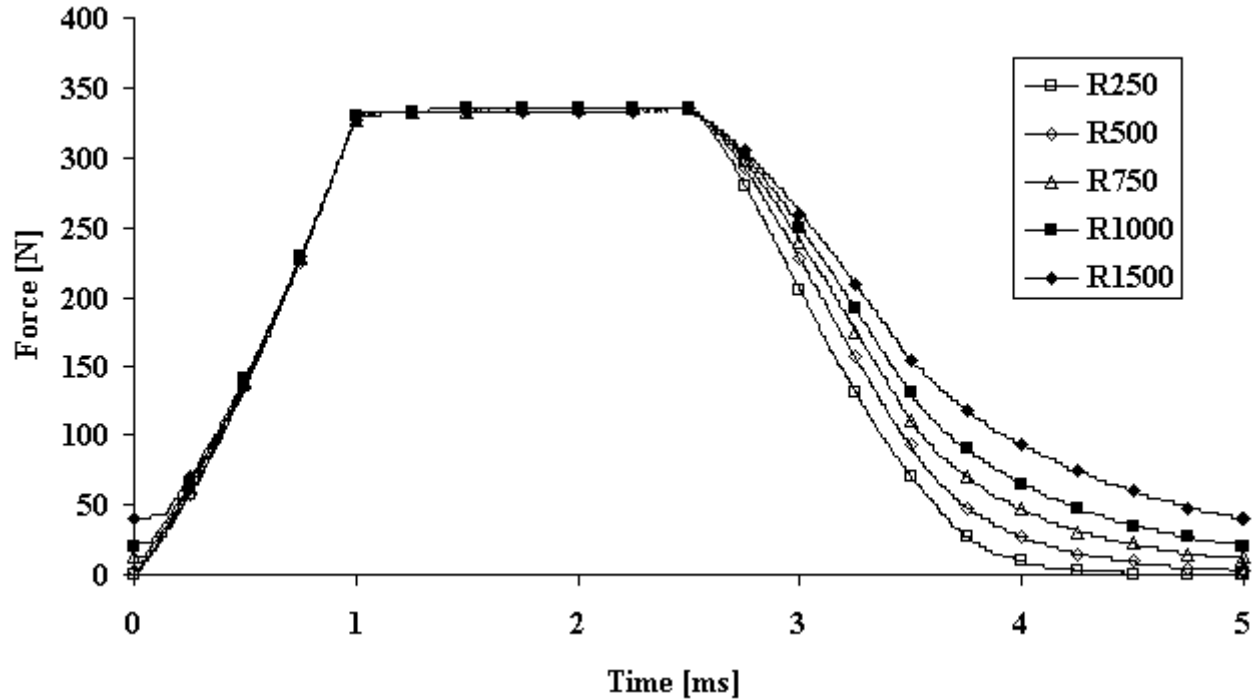


Figure 8. Experimental results showing clamping force vs. time for various resistances in the delay circuit acting on the falling edge of the voltage input.

6. ANALYSIS

The total restraining force on the moving member of a complementary inchworm actuator is obtained by adding the restraining forces of the two clamps. Fig. 9 shows the total restraining force as a function of common clamp voltage for the case of ideal complementary clamps where the force-voltage characteristics of the individual clamps are as shown in the right panels of Figs. 2a and 2b. It is assumed for simplicity that the clamps are fully complementary so that the magnitude of the F vs. V slopes for the two clamp types are the same. It is also assumed that $F_{\max\text{NU}}=F_{\max\text{NC}}=F_{\text{MAX}}$, $V_{\text{TNU}}=V_{\text{MAX}}/5$, and $V_{\text{TNC}}=V_{\text{MAX}}-V_{\text{TNU}}$. There is no common clamp voltage at which the total clamping force is zero, since the condition $V_{\text{TNC}}>V_{\text{TNU}}$ is satisfied. However the figure shows that the total restraining force is reduced for common clamp voltages that are intermediate between 0 and V_{MAX} . The reduction occurs because of the finite regions of the individual F vs. V characteristics where one clamp cannot compensate for force reduction of the other ($V<V_{\text{TNU}}$ for the NU clamp and $V>V_{\text{TNC}}$ for the NC clamp). These regions cannot be entirely removed from a practical design and we therefore expect that a complementary inchworm actuator with 2-channel control would ordinarily have a lower force drive capability than if the same actuator used 3-channel control to ensure that one clamp is fully on before the other begins to release. For the parameters chosen in this example, $F_{\text{MIN}}=0.75F_{\text{MAX}}$.

Fig. 10 shows the simulated total restraining force of the inchworm actuator as a function of time as the common clamp voltage is ramped from 0 to $V_{\text{MAX}}=200\text{V}$ at a rate of 200V/ms . Results for the downward ramp would appear the same in a fully complementary actuator. The response curve for the case when the delay circuit is not used has the same form as Fig. 9 but here the transition points t_{NU} and t_{NC} are the times when the input voltage is equal to V_{TNU} and V_{TNC} respectively. The other response curves show the effect of introducing the diode-shunted delay circuit and of using different values of R in the delay circuit. The initial rate of force reduction is reduced for the NC clamp due to the delay circuit and this is reflected in the reduced slope near $t=0$. The NU clamp begins to add to the total force at $t=t_{\text{NU}}$, since its delay circuit is bypassed on the rising portion of the voltage ramp. However V_{NC} is delayed in reaching V_{TNC} because of the delay circuit and consequently F_{NC} does not reach zero and the total force curve does not coincide with the NU curve until some time after $t=t_{\text{NC}}$. This point can be seen for the $R=250\Omega$ and $R=500\Omega$ curves but is off-scale for the $R=1000\Omega$ curve. In the latter case the total force exceeds F_{MAX} for a short period since the NC force has not yet reached

zero when the NU force first reaches F_{MAX} . It is important to ensure that the extender actuator is not triggered until the NC clamp has reached zero force and this means that R cannot be made arbitrarily large. However this condition can be easily satisfied while still increasing F_{MIN} to greater than 90% of F_{MAX} .

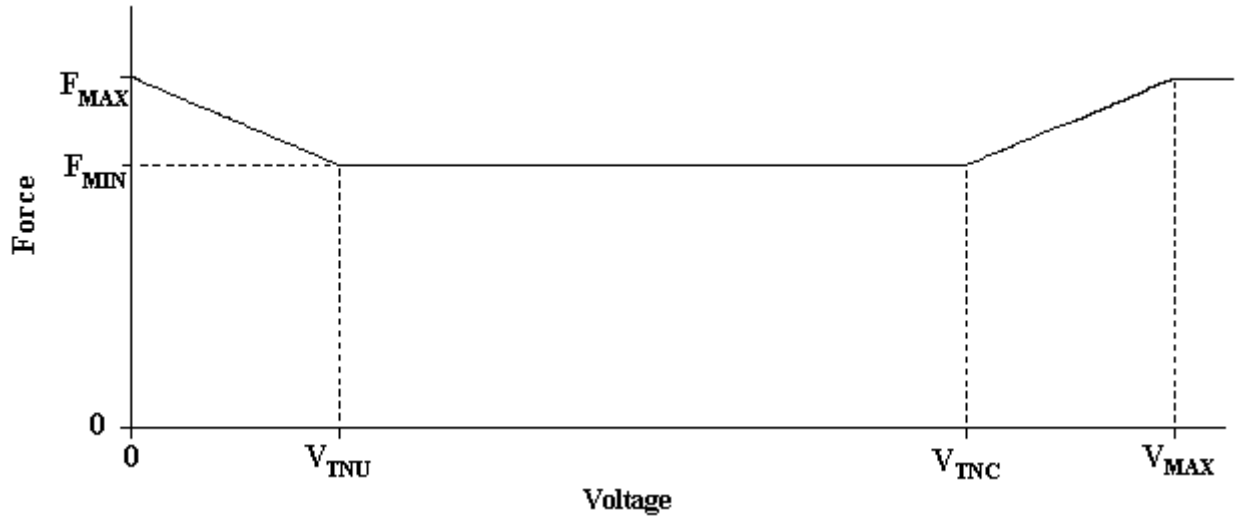


Figure 9. Total clamp force vs. voltage for complementary inchworm actuator.

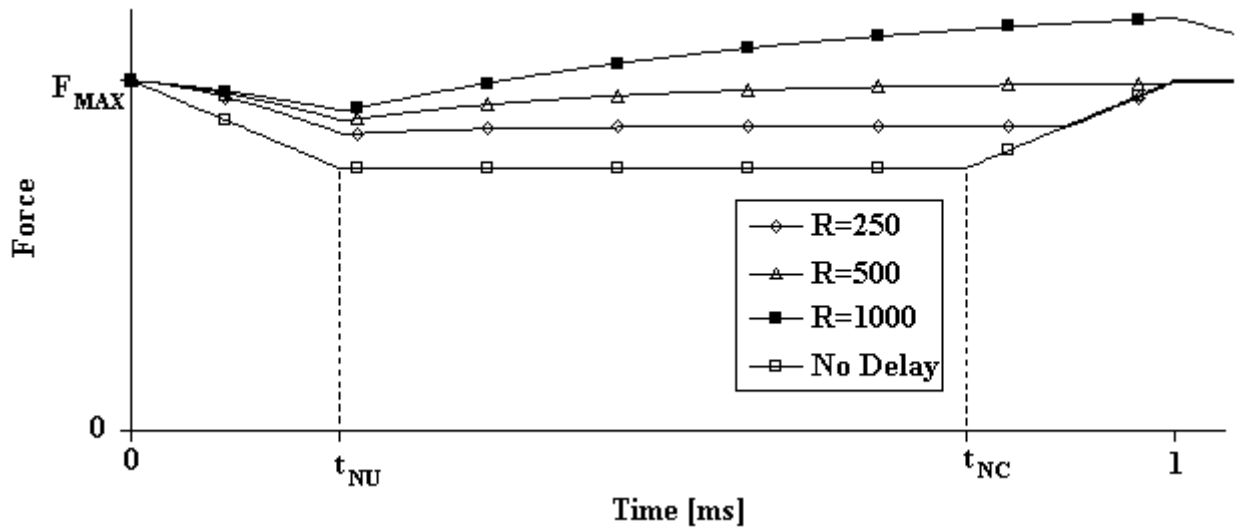


Figure 10. Simulated total clamp force vs. time for complementary inchworm actuator with and without diode-shunted delay circuit. The curves with delay circuit use $C=100nF$, $L=1mH$ and R values as shown.

7. CONCLUSIONS

Novel complementary clamp configurations for inchworm actuators have been described which allow one control signal to drive both clamps. This is achieved by designing the clamps so that one releases at high voltage and the other at low voltage. In the coarse positioning mode, the direction of motion depends on which edge of the common clamp signal the extender signal overlaps. A fine positioning mode can be realized with the common clamp voltage set to zero and continuous feedback control applied to the extender actuator.

A diode-shunted delay circuit has also been described which selectively slows the rate of unclamping relative to clamping. It has been shown by experiment and simulation that the circuit increases the actuator restraining force during the clamp switching transient. The complementary inchworm actuator with 2-channel control can achieve very close to the same force drive capability as a comparable inchworm actuator using 3-channel control.

ACKNOWLEDGMENT

This work was supported by the Canadian Space Agency under the STDP Program.

REFERENCES

1. B. Zhang and Z. Zhu, "Developing a linear piezomotor with nanometer resolution and high stiffness", *IEEE/ASME Transactions on Mechatronics*, **2**, 22-29, 1997.
2. R. Ben Mrad, A. Abhari and J. Zu, "A control methodology for an inchworm piezomotor", *Journal of Mechanical Systems and Signal Processing*, **17**, 457-71, 2003.
3. J. Kim; J-D. Kim and S-B Choi, "A Hybrid Inchworm Linear Motor", *Mechatronics*, **12**, 525-42, 2002.
4. A. Suleman, S. Burns, D. Waechter, R. Blacow, B. Yan and S.E. Prasad, "Flexural brake mechanism for inchworm actuator", *Proc. Canada-US CanSmart Workshop on Smart Materials and Structures*, Ed. G. Akhras, 125-36, Montreal, 2001.
5. R. Yeh, S. Hollar and K.S.J. Pister, "Single mask, large force, and large displacement electrostatic linear inchworm motors", *Journal of Microelectromechanical Systems*, **11**, 330-6, 2002.
6. A. Chandrakasan and R.W. Brodersen, eds., *Low-Power CMOS Design*, Wiley-IEEE Press, 1998.
7. S. Salisbury, D. Waechter, R. Ben Mrad, R. Blacow and E. Prasad, "Design tools for piezoelectric actuated inchworm positioners", *Proc. Canada-US CanSmart Workshop on Smart Materials and Structures*, Ed. G. Akhras, 169-75, Montreal, 2003.
8. PSPICE, Version 9.1, Cadence Design Systems Inc.